JOURNAL OF MOLECULAR SPECTROSCOPY **94**, 426–436 (1982)

The Millimeter and Submillimeter Spectrum of HO_2: The Effects of Unpaired Electronic Spin in a Light Asymmetric Rotor

ARTHUR CHARO AND FRANK C. DE LUCIA

Department of Physics, Duke University, Durham, North Carolina 27706

An extensive data set for the transient species HO_2 was acquired in the spectral region between 150 and 550 GHz. The complex spectrum of this light asymmetric rotor with unpaired electronic spin and nuclear hyperfine interactions was analyzed and fit to within experimental uncertainty (<0.1 MHz). This work provides, either by direct measurement or well-founded calculation, a map of the rotational transition frequencies of HO_2 over a wide range of states.

I. INTRODUCTION

The hydroperoxy radical, HO_2, is a short-lived species that plays a prominent role as a transient intermediate in a myriad of chemical reactions. It is, for example, often involved in radical chain reactions such as those believed to occur in the oxidation of hydrocarbons (*1*). In addition, there is continuing interest in the interaction of HO_2 within ozone formation and destruction cycles (*2*). Because HO_2 is a light asymmetric rotor with unpaired electronic spin, it is also of considerable interest to spectroscopists as a testing ground for theoretical models.

The acquisition of a substantial data base for HO_2 represents a significant experimental challenge because of the reactivity of the species and because most of its rotational spectrum falls in the shorter millimeter and submillimeter spectral region. The first investigations of the rotational spectrum of HO_2 were by Radford *et al.* (*3*) and Hougen *et al.* (*4*), using far-infrared laser magnetic resonance. By use of the molecular constants determined by this work, Beers and Howard (*5*) were able to observe the 1_{00}–0_{00} transition of HO_2 at 65 GHz in a microwave absorption experiment. Saito (*6*) measured all six of the *a*-type $N = 2 \leftarrow 1$ transitions and eight *b*-type transitions in a microwave absorption experiment between 30 and 140 GHz. The EPR spectrum of HO_2 was studied by Barnes *et al.* (*7*), who also performed a combined analysis of microwave, EPR, and LMR data. In this work are reported the measurement of 87 new transitions (many of which have resolvable hyperfine structure) in the spectral region between 150 and 550 GHz and the detailed analysis of these data. The extension of the microwave data to higher values of the rotational quantum numbers N and K (26 and 4, respectively) provides new information that is used to refine estimates of the spectral constants necessary for the analysis of this complex spectroscopic species. In addition, the millimeter and submillimeter wave data provided in this work should allow the remote measurement of HO_2 in the upper atmosphere (*8*) and its possible detection in the interstellar medium.

0022-2852/82/080426-11$02.00/0

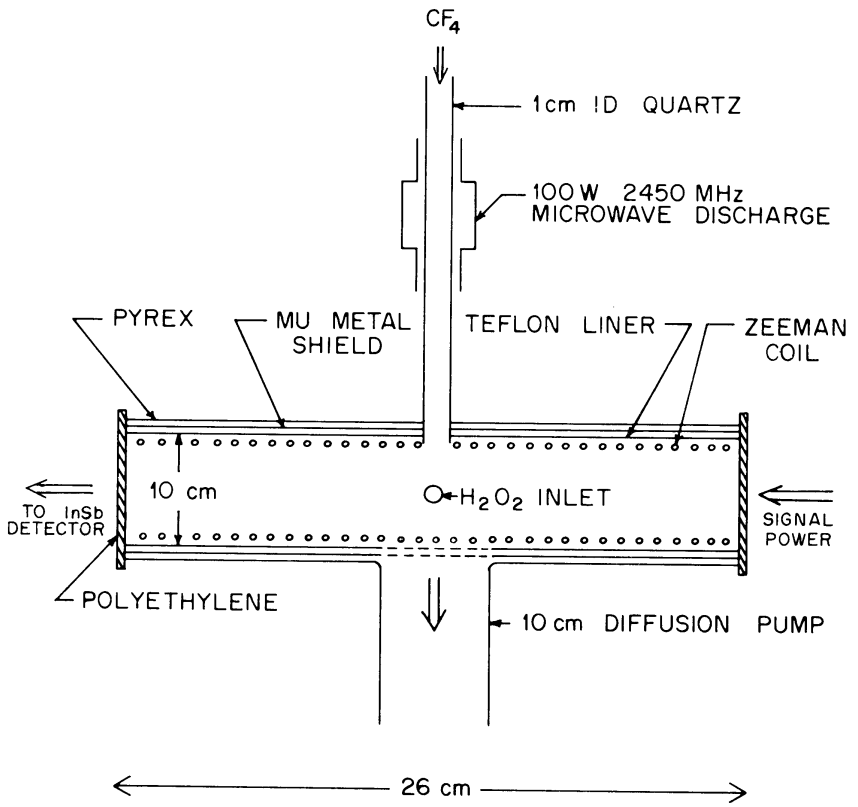

FIG. 1. Absorption cell for the production of HO_2.

II. EXPERIMENTAL DETAILS

We have previously described the details of our millimeter and submillimeter spectroscopic technique (*9*). Briefly, a phase-locked klystron in the 50-GHz region is used to drive a crystal harmonic generator, the output of which is focused by quasi-optical techniques through the sample cell and detected by a 1.4 K InSb detector. The absorption cell used for most of the measurements is shown in Fig. 1. HO_2 is produced in the cell from the reaction of the discharge products of a CF_4 discharge with H_2O_2 in a fast flow configuration. Ninety percent pure hydrogen peroxide was obtained from the FMC Corporation and was used without further purification. HO_2 was produced under a broad range of conditions. Typical operating conditions (with the microwave discharge turned off) as recorded by an NRC 501 thermocouple mounted at the diffusion pump were $\sim 20\ \mu$ CF_4 and $\sim 1\ \mu$ H_2O_2. The use of a buffer gas such as helium did not enhance HO_2 production.

Although the stronger transitions of HO_2 could be observed in real time on an oscilloscope, nearly all of the measurements were made with phase-locked klystrons and lock-in detection with a time constant of one second. Modulation for this phase-sensitive detection was provided by either Zeeman modulation or by frequency modulation of the klystron. Zeeman modulation was particularly useful below ~ 300 GHz, where baseline effects are severe. However, modulation broadening of spectral lines was frequently unavoidable.

III. THEORY

HO_2 is a light, nearly prolate, asymmetric rotor with one unpaired electron and one nonzero nuclear spin. Thus, an appropriate angular momentum coupling scheme is

$$\mathbf{N} + \mathbf{S} = \mathbf{J}, \tag{1a}$$

$$\mathbf{J} + \mathbf{I} = \mathbf{F}, \tag{1b}$$

where **N** is the rotational angular momentum, **S** the electron spin angular momentum, **I** the nuclear spin angular momentum, and **J** and **F** are defined by the coupling scheme.

The effective zero field Hamiltonian can be written as

$$\mathscr{H}_{\text{eff}} = \mathscr{H}_{\text{r}} + \mathscr{H}_{\text{cd}} + \mathscr{H}_{\text{sr}} + \mathscr{H}_{\text{srcd}} + \mathscr{H}_{\text{hfs}} , \tag{2}$$

where $\mathscr{H}_{\text{r}}$ is the rigid asymmetric rotor Hamiltonian, $\mathscr{H}_{\text{cd}}$ contains the quartic and sextic centrifugal distortion corrections to $\mathscr{H}_{\text{r}}$, $\mathscr{H}_{\text{sr}}$ is the electron spin–rotation interaction, $\mathscr{H}_{\text{srcd}}$ contains the centrifugal distortion corrections to $\mathscr{H}_{\text{sr}}$, and $\mathscr{H}_{\text{hfs}}$ is the magnetic hyperfine interaction between the unpaired electron and the hydrogen nucleus.

The terms in this Hamiltonian have been discussed by a number of authors. As in our earlier work on light asymmetric rotors (*10*, *11*), we have adopted Watson's (*12*) *A*-reduced Hamiltonian for $\mathscr{H}_{\text{r}}$ and $\mathscr{H}_{\text{cd}}$. The effective spin–rotation Hamiltonian has been given by Van Vleck (*13*) and explicit forms of the matrix elements of $\mathscr{H}_{\text{sr}}$ have been given by Raynes (*14*), Woodman (*15*), and Bowater *et al.* (*16*). Brown and Sears (*17*) have shown for molecules with only a single plane of symmetry that there are four, not five, determinable quadratic spin–rotation parameters. In the principal axis system of the molecule these may be taken to be ϵ_{aa}, ϵ_{bb}, ϵ_{cc}, and $\epsilon_{ab} + \epsilon_{ba}$. Brown and Sears have also presented both *A*- and *S*-reduced Hamiltonians for $\mathscr{H}_{\text{srcd}}$. These reductions are analogous to the *A*- and *S*-reduced forms of $\mathscr{H}_{\text{cd}}$ presented by Watson (*12*).

For the analysis of HO_2 presented in this paper, we adopt the *A*-reduced form of $\mathscr{H}_{\text{r}}$ and $\mathscr{H}_{\text{cd}}$. This is the same choice that we have made previously in our extensive work on singlet light asymmetric rotors. A consistent construction of the Hamiltonian matrix requires, therefore, that $\mathscr{H}_{\text{sr}}$ and $\mathscr{H}_{\text{srcd}}$ also be formulated in the *A*-reduced form of Brown and Sears (*17*).

The coupling scheme of Eq. (1) defines the basis in which the Hamiltonian matrix is closest to diagonal form. In the absence of external fields, F is a good quantum number and, in principle, the matrix elements for HO_2 could be assembled in blocks characterized by a common value of F and diagonalized to provide energy levels. Unfortunately, this direct approach is rather uneconomical because the diagonalization of a large number of matricies of dimension $\sim$200 would be required. Thus, approximation methods are required.

First, it should be noted that although the spin–rotation energies are not small in comparison to the rotational energies (spin splittings of 50 GHz are not uncommon in HO_2), we can separate the hyperfine Hamiltonian, $\mathscr{H}_{\text{hfs}}$, from the total Hamiltonian because

$$E_{\text{rot}} \gtrsim E_{\text{sr}} \gg E_{\text{hfs}} . \tag{3}$$

TABLE I

Observed Transitions of HO_2 (MHz)

Rotational Transition	J'←J	F'←F	Observed Frequency
3(0, 3)← 2(0, 2)	5/2← 3/2	3← 2	195629.55
		2← 1	195628.34
3(0, 3)← 2(0, 2)	7/2← 5/2	4← 3	195423.56
		3← 2	195422.64
3(1, 2)← 2(1, 1)	5/2← 3/2	3← 2	193940.83
		2← 1	193939.56
		2← 2	193937.06
3(1, 2)← 2(1, 1)	7/2← 5/2	4← 3	200617.47
		3← 2	200615.72
3(1, 3)← 2(1, 2)	5/2← 3/2	3← 2	188350.71
		2← 1	188351.58
3(1, 3)← 2(1, 2)	7/2← 5/2	4← 3	195220.22
		3← 2	195219.25
3(1, 3)← 4(0, 4)	5/2← 7/2	3← 4	321833.31
		2← 3	321826.88
3(1, 3)← 4(0, 4)	7/2← 9/2	4← 5	303438.00
		3← 4	303441.59
3(2, 1)← 2(2, 0)	5/2← 3/2	3← 2	184212.64
		2← 1	184214.87
3(2, 1)← 2(2, 0)	7/2← 5/2	4← 3	202888.18
		3← 2	202885.94
3(2, 2)← 2(2, 1)	5/2← 3/2	3← 2	184194.55
		2← 1	184196.76
3(2, 2)← 2(2, 1)	7/2← 5/2	4← 3	202872.19
		3← 2	202869.98
4(0, 4)← 3(0, 3)	7/2← 5/2	4← 3	260770.14
		3← 2	
4(0, 4)← 3(0, 3)	9/2← 7/2	5← 4	260565.86
		4← 3	
4(1, 3)← 3(1, 2)	7/2← 5/2	4← 3	262004.09
		3← 2	
4(1, 3)← 3(1, 2)	9/2← 7/2	5← 4	265770.21
		4← 3	265769.20
4(1, 4)← 3(1, 3)	7/2← 5/2	4← 3	254551.53
		3← 2	
4(1, 4)← 3(1, 3)	9/2← 7/2	5← 4	258522.94
		4← 3	
4(1, 4)← 5(0, 5)	7/2← 9/2	4← 5	250502.47
		3← 4	250496.86
4(1, 4)← 5(0, 5)	9/2←11/2	5← 6	236280.92
		4← 5	236284.42
4(2, 2)← 3(2, 1)	7/2← 5/2	4← 3	253233.72
		3← 2	
4(2, 2)← 3(2, 1)	9/2← 7/2	5← 4	265731.52
		4← 3	
4(2, 3)← 3(2, 2)	7/2← 5/2	4← 3	253189.10
		3← 2	
4(2, 3)← 3(2, 2)	9/2← 7/2	5← 4	265690.53
		4← 3	
4(3, 2)← 3(3, 1) 4(3, 1)← 3(3, 0)	7/2← 5/2	4← 3	248431.39
		3← 2	248433.15
4(3, 2)← 3(3, 1) 4(3, 1)← 3(3, 0)	9/2← 7/2	5← 4	269500.65
		4← 3	269498.83
5(0, 5)← 4(0, 4)	9/2← 7/2	5← 4	325882.22
		4← 3	

TABLE I—*Continued*

Rotational Transition	J'←J	F'←F	Observed Frequency
5(0, 5)← 4(0, 4)	11/2← 9/2	6← 5 5← 4	325680.17
5(1, 4)← 4(1, 3)	9/2← 7/2	5← 4 4← 3	328995.55
5(1, 4)← 4(1, 3)	11/2← 9/2	6← 5 5← 4	331333.01
5(1, 5)← 4(1, 4)	9/2← 7/2	5← 4 4← 3	316694.62
5(1, 5)← 4(1, 4)	11/2← 9/2	6← 5 5← 4	322242.67
5(1, 5)← 6(0, 6)	9/2←11/2	5← 6 4← 5	179238.50 179233.33
5(1, 5)← 6(0, 6)	11/2←13/2	6← 7 5← 6	167765.03 167768.28
5(2, 3)← 4(2, 2)	9/2← 7/2	5← 4 4← 3	320720.20
5(2, 3)← 4(2, 2)	11/2← 9/2	6← 5 5← 4	329456.21
5(2, 4)← 4(2, 3)	9/2← 7/2	5← 4 4← 3	320631.39
5(2, 4)← 4(2, 3)	11/2← 9/2	6← 5 5← 4	329373.04
5(3, 2)← 4(3, 1) 5(3, 3)← 4(3, 2)	9/2← 7/2	5← 4 4← 3	316548.27
5(3, 2)← 4(3, 1) 5(3, 3)← 4(3, 2)	11/2← 9/2	6← 5 5← 4	332466.93
5(4, 1)← 4(4, 0) 5(4, 2)← 4(4, 1)	9/2← 7/2	5← 4 4← 3	312884.54 312886.24
5(4, 1)← 4(4, 0) 5(4, 2)← 4(4, 1)	11/2← 9/2	6← 5 5← 4	335323.63 335321.98
6(0, 6)← 5(0, 5)	11/2← 9/2	6← 5 5← 4	390958.21
6(0, 6)← 5(0, 5)	13/2←11/2	7← 6 6← 5	390758.87
6(1, 5)← 5(1, 4)	11/2← 9/2	6← 5 5← 4	395535.68
6(1, 5)← 5(1, 4)	13/2←11/2	7← 6 6← 5	397077.70
6(1, 6)← 5(1, 5)	11/2← 9/2	6← 5 5← 4	384392.68
6(1, 6)← 5(1, 5)	13/2←11/2	7← 6 6← 5	386147.31
6(2, 4)← 5(2, 3)	11/2← 9/2	6← 5 5← 4	387333.95
6(2, 4)← 5(2, 3)	13/2←11/2	7← 6 6← 5	393690.63
6(2, 5)← 5(2, 4)	11/2← 9/2	6← 5 5← 4	387178.99
6(2, 5)← 5(2, 4)	13/2←11/2	7← 6 6← 5	393543.30
6(3, 3)← 5(3, 2) 6(3, 4)← 5(3, 3)	13/2←11/2	7← 6 6← 5	396034.05
6(4, 2)← 5(4, 1) 6(4, 3)← 5(4, 2)	11/2← 9/2	6← 5 5← 4	380375.03
6(4, 2)← 5(4, 1) 6(4, 3)← 5(4, 2)	13/2←11/2	7← 6 6← 5	398470.75
7(0, 7)← 6(0, 6)	13/2←11/2	7← 6 6← 5	455990.94

TABLE I—*Continued*

Rotational Transition	J'←J	F'←F	Observed Frequency
7(0, 7)← 6(0, 6)	15/2←13/2	8← 7 7← 6	455794.60
7(1, 6)← 6(1, 5)	13/2←11/2	7← 6 6← 5	461847.69
7(1, 7)← 6(1, 6)	13/2←11/2	7← 6 6← 5	448867.53
7(1, 7)← 6(1, 6)	15/2←13/2	8← 7 7← 6	450136.82
7(2, 5)← 6(2, 4)	13/2←11/2	7← 6 6← 5	453447.97
7(2, 5)← 6(2, 4)	15/2←13/2	8← 7 7← 6	458231.55
7(2, 6)← 6(2, 5)	13/2←11/2	7← 6 6← 5	453200.48
7(2, 6)← 6(2, 5)	15/2←13/2	8← 7 7← 6	457994.45
7(3, 4)← 6(3, 3) 7(3, 5)← 6(3, 4)	13/2←11/2	7← 6 6← 5	450374.25
7(3, 4)← 6(3, 3) 7(3, 5)← 6(3, 4)	15/2←13/2	8← 7 7← 6	460006.04
7(4, 3)← 6(4, 2) 7(4, 4)← 6(4, 3)	13/2←11/2	7← 6 6← 5	447289.85
7(4, 3)← 6(4, 2) 7(4, 4)← 6(4, 3)	15/2←13/2	8← 7 7← 6	462034.53
8(0, 8)← 7(0, 7)	15/2←13/2	8← 7 7← 6	520972.33
8(0, 8)← 7(0, 7)	17/2←15/2	9← 8 8← 7	520780.45
11(0,11)←10(1,10)	21/2←19/2	11←10 10← 9	184373.81 183378.30
11(0,11)←10(1,10)	23/2←21/2	12←11 11←10	189600.00 189596.64
12(0,12)←11(1,11)	23/2←21/2	12←11 11←10	258872.75 258877.05
12(0,12)←11(1,11)	25/2←23/2	13←12 12←11	263460.52 263457.21
13(0,13)←12(1,12)	25/2←23/2	13←12 12←11	333936.32 333940.27
13(0,13)←12(1,12)	27/2←25/2	14←13 13←12	337977.84 337974.55
17(2,16)←18(1,17)	33/2←35/2	17←18 16←17	408522.19 408517.95
17(2,16)←18(1,17)	35/2←37/2	18←19 17←18	326358.47 326354.31
18(2,17)←19(1,18)	35/2←37/2	18←19 17←18	399022.02 399025.60
18(2,17)←19(1,18)	37/2←39/2	19←20 18←19	317603.71 317607.23
19(2,18)←20(1,19)	37/2←39/2	19←20 18←19	243474.69 243470.60
19(2,18)←20(1,19)	39/2←41/2	20←21 19←20	235399.96 235403.51
25(1,24)←24(2,23)	51/2←49/2	26←25 25←24	186594.26 186590.82
26(1,25)←25(2,24)	51/2←49/2	26←25 25←24	268124.79 268128.81
26(1,25)←25(2,24)	53/2←51/2	27←26 26←25	273016.56 273013.19

Thus, to an excellent approximation $\mathscr{H}_{\text{hfs}}$ can be separated from the rest of the Hamiltonian and treated by perturbation theory. The matrix elements of $\mathscr{H}_0 \equiv \mathscr{H} - \mathscr{H}_{\text{hfs}}$ are diagonal in J, and the calculation of asymmetric rotor energy levels, apart from hyperfine contributions, may be accomplished by diagonalizing only matrices diagonal in J. The hyperfine energies in the asymmetric rotor basis may then be calculated using the eigenvectors that diagonalize $\mathscr{H}_0$ and matrix elements evaluated in the basis of Eq. (1). This calculation neglects matrix elements of $\mathscr{H}_{\text{hfs}}$ which are off diagonal in J. The contributions of these elements are negligible except for levels that are diagonal in N and K for $K = 0$. A separate second-order calculation of the energy contribution of these matrix elements completes the decoupling of $\mathscr{H}_{\text{hfs}}$ from $\mathscr{H}$.

After the removal of the hyperfine structure, each of the remaining J blocks has dimension $4J + 2$. The problem can be reduced further by performing a modified Wang transformation, appropriate for doublet states, as suggested by Raynes (*14*). This reduction results in four submatricies of dimension $(J + 1/2)$. Unfortunately, for molecules that lack C_{2v} symmetry, $\epsilon_{ab} + \epsilon_{ba} \neq 0$, and matrix elements of this term couple these submatricies. However, since this term is relatively small, it too can be included via perturbation theory.

IV. RESULTS AND DISCUSSION

Table I shows the results of our experimental observations. In many cases the nuclear hyperfine splittings are smaller than the Doppler- or modulation-broadened width of the transition and only a single observed frequency is listed. In other cases, the asymmetry splittings are also less than the Doppler width and again only a single observed frequency is listed.

For the purposes of our analysis, the observed transitions of Table I must be converted to hypothetical unsplit frequencies by removal of the hyperfine energies. Since the hyperfine splittings are largest at small N, and since the hyperfine constants have been accurately calculated by Barnes *et al.* (*7*) from the low N data of Saito (*6*), we use these parameters to calculate the hyperfine contributions to our observed lines. In those cases for which we observe a resolved doublet, these contributions are simply subtracted and averaged to give a single unsplit frequency. We find that our predictions of the splittings agree to within the experimental uncertainty of our observations. For unresolved or marginally resolved transitions the predictions of an intensity weighted spectrum are used to determine the unsplit frequency.

Because our factorization removes the contributions of the $\epsilon_{ab} + \epsilon_{ba}$ term, these contributions must be calculated separately. Except for those levels where the contribution is largest (this occurs where $E_{N+1,K_{-1}} \sim E_{N,K_{-1}+1}$) calculations based upon second-order perturbation theory are correct to within experimental uncertainty. However, at the points where the energy denominator is relatively small, third-order perturbation theory predicts additional corrections on the order of 1 MHz. In these cases an exact diagonalization of the unfactored matrix was carried out and appropriate corrections to second-order theory included. These corrections

TABLE II

Transitions of HO_2 with Hyperfine Structure Removed (MHz)

Rotational Transition	$J' \leftarrow J$	Observed [a] Frequency	Obs. - Cal.
1(0, 1) - 0(0, 0)	1/2 - 1/2	65392.10	0.02
1(0, 1) - 0(0, 0)	3/2 - 1/2	65081.39	-0.05
2(0, 2) - 1(0, 1)	3/2 - 1/2	130465.71	-0.18
2(0, 2) - 1(0, 1)	5/2 - 3/2	130259.89	0.37[b]
2(1, 1) - 1(1, 0)	3/2 - 1/2	122858.53	0.02
2(1, 1) - 1(1, 0)	5/2 - 3/2	136495.10	0.11
2(1, 2) - 1(1, 1)	3/2 - 1/2	119153.00	-0.15
2(1, 2) - 1(1, 1)	5/2 - 3/2	132961.83	0.02
3(0, 3) - 2(0, 2)	5/2 - 3/2	195628.79	0.02
3(0, 3) - 2(0, 2)	7/2 - 5/2	195423.42	-0.03
3(1, 2) - 2(1, 1)	5/2 - 3/2	193940.19	-0.05
3(1, 2) - 2(1, 1)	7/2 - 5/2	200617.00	-0.02
3(1, 3) - 2(1, 2)	5/2 - 3/2	188350.39	-0.05
3(1, 3) - 2(1, 2)	7/2 - 5/2	195220.16	0.10
3(1, 3) - 4(0, 4)	5/2 - 7/2	321830.93	0.03
3(1, 3) - 4(0, 4)	7/2 - 9/2	303439.30	-0.14
3(2, 2) - 2(2, 1)	5/2 - 3/2	184194.87	-0.01
3(2, 2) - 2(2, 1)	7/2 - 5/2	202871.61	-0.08
3(2, 1) - 2(2, 0)	5/2 - 3/2	184212.97	-0.00
3(2, 1) - 2(2, 0)	7/2 - 5/2	202887.58	-0.04
4(0, 4) - 3(0, 3)	7/2 - 5/2	260769.98	0.09
4(0, 4) - 3(0, 3)	9/2 - 7/2	260566.01	-0.06
4(1, 3) - 3(1, 2)	7/2 - 5/2	262003.99	0.09
4(1, 3) - 3(1, 2)	9/2 - 7/2	265769.91	0.01
4(1, 4) - 3(1, 3)	7/2 - 5/2	254551.20	-0.09
4(1, 4) - 3(1, 3)	9/2 - 7/2	258523.15	0.02
4(1, 4) - 5(0, 5)	7/2 - 9/2	250500.24	0.13
4(1, 4) - 5(0, 5)	9/2 - 11/2	236282.30	-0.06
4(2, 2) - 3(2, 1)	7/2 - 5/2	253233.48	0.00
4(2, 2) - 3(2, 1)	9/2 - 7/2	265731.71	-0.05
4(2, 3) - 3(2, 2)	7/2 - 5/2	253188.86	-0.01
4(2, 3) - 3(2, 2)	9/2 - 7/2	265690.72	-0.02
4(3, 1) - 3(3, 0) 4(3, 2) - 3(3, 1)	7/2 - 5/2	248431.83	0.18
4(3, 1) - 3(3, 0) 4(3, 2) - 3(3, 1)	9/2 - 7/2	269500.06	-0.15
5(0, 5) - 4(0, 4)	9/2 - 7/2	325882.12	0.03
5(0, 5) - 4(0, 4)	11/2 - 9/2	325680.26	0.05
5(1, 4) - 4(1, 3)	9/2 - 7/2	328995.49	-0.01
5(1, 4) - 4(1, 3)	11/2 - 9/2	331333.10	0.01
5(1, 5) - 4(1, 4)	9/2 - 7/2	319694.43	0.00
5(1, 5) - 4(1, 4)	11/2 - 9/2	322242.81	0.07
5(1, 5) - 6(0, 6)	9/2 - 11/2	179236.34	-0.03
5(1, 5) - 6(0, 6)	11/2 - 13/2	167766.36	-0.00
5(2, 3) - 4(2, 2)	9/2 - 7/2	320720.06	0.03
5(2, 3) - 4(2, 2)	11/2 - 9/2	329456.33	-0.21
5(2, 4) - 4(2, 3)	9/2 - 7/2	320631.25	0.03
5(2, 4) - 4(2, 3)	11/2 - 9/2	329373.16	0.01

[a] Observed transitions below 150 GHz from reference 6.

[b] Line omitted from fit.

TABLE II—*Continued*

Rotational Transition	J′ ← J	Observed Frequency	Obs. - Cal.
5(3, 2) - 4(3, 1) 5(3, 3) - 4(3, 2)	9/2 - 7/2	316548.11	0.23
5(3, 2) - 4(3, 1) 5(3, 3) - 4(3, 2)	11/2 - 9/2	332467.06	-0.06
5(4, 1) - 4(4, 0) 5(4, 2) - 4(4, 1)	9/2 - 7/2	312885.11	-0.10
5(4, 1) - 4(4, 0) 5(4, 2) - 4(4, 1)	11/2 - 9/2	335323.02	0.14
6(0, 6) - 5(0, 5)	11/2 - 9/2	390958.10	-0.06
6(0, 6) - 5(0, 5)	13/2 - 11/2	390758.93	0.19
6(1, 5) - 5(1, 4)	11/2 - 9/2	395535.64	0.09
6(1, 5) - 5(1, 4)	13/2 - 11/2	397077.76	-0.02
6(1, 6) - 5(1, 5)	11/2 - 9/2	384392.55	-0.15
6(1, 6) - 5(1, 5)	13/2 - 11/2	386147.41	0.06
6(1, 6) - 7(0, 7)	11/2 - 13/2	107638.20	-0.04
6(1, 6) - 7(0, 7)	13/2 - 15/2	98119.24	0.08
6(2, 4) - 5(2, 3)	11/2 - 9/2	387333.86	-0.01
6(2, 4) - 5(2, 3)	13/2 - 11/2	393690.71	-0.00
6(2, 5) - 5(2, 4)	11/2 - 9/2	387178.90	0.05
6(2, 5) - 5(2, 4)	13/2 - 11/2	393543.38	0.01
6(3, 3) - 5(3, 2) 6(3, 4) - 5(3, 3)	13/2 - 11/2	396034.14	-0.15
6(4, 2) - 5(4, 1) 6(4, 3) - 5(4, 2)	11/2 - 9/2	380374.91	-0.14
6(4, 2) - 5(4, 1) 6(4, 3) - 5(4, 2)	13/2 - 11/2	398470.84	0.10
7(0, 7) - 6(0, 6)	13/2 - 11/2	455990.89	0.06
7(0, 7) - 6(0, 6)	15/2 - 13/2	455794.65	0.11
7(1, 6) - 6(1, 5)	13/2 - 11/2	461847.65	-0.21
7(1, 7) - 6(1, 6)	13/2 - 11/2	448867.44	0.06
7(1, 7) - 6(1, 6)	15/2 - 13/2	450136.89	-0.17
7(1, 7) - 8(0, 8)	13/2 - 15/2	35533.42	0.07
7(1, 7) - 8(0, 8)	15/2 - 17/2	27475.76	0.06
7(2, 5) - 6(2, 4)	13/2 - 11/2	453447.91	0.01
7(2, 5) - 6(2, 4)	15/2 - 13/2	458231.61	-0.06
7(2, 6) - 6(2, 5)	13/2 - 11/2	453200.42	0.06
7(2, 6) - 6(2, 5)	15/2 - 13/2	457994.51	0.03
7(3, 4) - 6(3, 3) 7(3, 5) - 6(3, 4)	13/2 - 11/2	450374.18	0.17
7(3, 4) - 6(3, 3) 7(3, 5) - 6(3, 4)	15/2 - 13/2	460006.10	-0.05
7(4, 3) - 6(4, 2) 7(4, 4) - 6(4, 3)	13/2 - 11/2	447289.77	-0.06
7(4, 3) - 6(4, 2) 7(4, 4) - 6(4, 3)	15/2 - 13/2	462034.60	0.02
8(0, 8) - 7(0, 7)	15/2 - 13/2	520972.30	0.04
8(0, 8) - 7(0, 7)	17/2 - 15/2	520780.49	-0.04
9(0, 9) - 8(1, 8)	17/2 - 15/2	37140.37	0.03
9(0, 9) - 8(1, 8)	19/2 - 17/2	44071.51	0.04
10(0, 10) - 9(1, 9)	19/2 - 17/2	110474.36	0.10
10(0, 10) - 9(1, 9)	21/2 - 19/2	116450.23	0.03
11(0, 11) - 10(1, 10)	21/2 - 19/2	184375.88	-0.10
11(0, 11) - 10(1, 10)	23/2 - 21/2	189598.46	-0.02
12(0, 12) - 11(1, 11)	23/2 - 21/2	258874.74	0.00
12(0, 12) - 11(1, 11)	25/2 - 23/2	263459.00	0.00

TABLE II—*Continued*

Rotational Transition	$J' \leftarrow J$	Observed Frequency	Obs. - Cal.
13(0, 13) - 12(1, 12)	25/2 - 23/2	333938.15	-0.04
13(0, 13) - 12(1, 12)	27/2 - 25/2	337976.31	0.04
17(2, 16) - 18(1, 17)	33/2 - 35/2	408520.14	-0.07
17(2, 16) - 18(1, 17)	35/2 - 37/2	399023.76	0.09
18(2, 17) - 19(1, 18)	35/2 - 37/2	326356.45	-0.00
18(2, 17) - 19(1, 18)	37/2 - 39/2	317605.41	0.02
19(2, 18) - 20(1, 19)	37/2 - 39/2	243472.70	0.02
19(2, 18) - 20(1, 19)	39/2 - 41/2	235401.69	-0.05
25(1, 24) - 24(2, 23)	51/2 - 49/2	186592.58	0.05
26(1, 25) - 25(2, 24)	51/2 - 49/2	268126.76	-0.01
26(1, 25) - 25(2, 24)	53/2 - 51/2	273014.91	-0.03

are both small and relatively insensitive to the other parameters and do not require inclusion in the iterative procedures.

Table II shows the data set that is the basis for our rotation and spin–rotation analysis and Table III shows the spectral constants that result from this analysis. Our large data set makes possible the calculation of these constants with good redundancy. Additional high-order terms (a full set of sextic rotational parameters and a full set of quartic spin–rotational parameters) have been tested and found to be unnecessary. The selection of constants to be retained have been made on the basis of criteria that we have previously discussed (*9*, *10*). A direct comparison of our results with those of Barnes *et al.* (*7*) is not possible both because of the

TABLE III

Spectral Constants of HO_2 (MHz)

Constant	Value	σ	Constant	Value	σ
A	610273.223	0.056	ε_{aa}	-49571.409	0.143
B	33517.816	0.051	ε_{bb}	-422.755	0.060
C	31667.654	0.051	ε_{cc}	8.605	0.060
			$\varepsilon_{ab}+\varepsilon_{ba}$	0.3879	0.0003
Δ_N	0.11693	0.00005			
Δ_{NK}	3.44552	0.00077	Δ^S_{NK}	0.1261	0.0022
Δ_K	123.572	0.028	Δ^S_K	23.061	0.020
δ_N	0.00613	0.00002			
δ_K	2.017	0.026	δ^S_K	0.079	0.018
$H_{NK}\cdot(10^5)$	2.29	0.57			
$H_{KN}\cdot(10^3)$	1.051	0.04			
$H_K\cdot(10^2)$	9.69	a			

(RMS deviation of fit = 0.084 MHz.)

[a] Fixed at the LMR value of reference 7.

different reductions used and because different high-order terms were retained in the Hamiltonian. However, once the S-reduced constants of Barnes *et al.* are converted to the A-reduced form (*12*), the agreements are satisfactory.

We have recently completed a study of the spectroscopically similar molecule NO_2 (*18*). However, a number of differences exist between the two species that lead us to a substantially different analysis strategy. In HO_2 we are able to effectively separate the nuclear hyperfine analysis from the rotation and spin–rotation analysis because in general $E_{sr} \gg E_{hfs}$. However, in NO_2 this is not true for many states and the dimensionality of the problem must be increased to include F quantum numbers. Furthermore, because NO_2 is both heavier and a stable species, the NO_2 data set extends to $J = 50$. On the other hand, ϵ_{aa} for NO_2 is much smaller than in HO_2, thereby reducing the coupling between adjacent N blocks. Thus, our approach for NO_2 was to include the hyperfine structure by diagonalization of F blocks, but to truncate these blocks in K (to solve the high J problem) and N (because of the smaller N coupling). By elimination of hyperfine structure, these two approximations may be cross-checked and we find their results to be virtually identical. That the NO_2 approximation holds for the HO_2 problem is perhaps not surprising because our truncated blocks are still rather large.

ACKNOWLEDGMENTS

We would like to thank Professor M. Mizushima for helpful discussions about hyperfine theory. Support for this work was provided by NASA Grant NSG-7540.

RECEIVED: March 19, 1982

REFERENCES

1. N. N. SEMENOV, *in* "Photochemistry and Reaction Kinetics" (P. G. Ashmore, Ed.), Cambridge Univ. Press, New York, 1967.
2. National Research Council, "Ozone and Other Photochemical Oxidants," National Academy of Sciences, Washington, D. C., 1977.
3. H. E. RADFORD, K. M. EVENSON, AND C. J. HOWARD, *J. Chem. Phys.* **60,** 3178–3183 (1974).
4. J. T. HOUGEN, H. E. RADFORD, K. M. EVENSON, AND C. J. HOWARD, *J. Mol. Spectrosc.* **56,** 210–228 (1975).
5. Y. BEERS AND C. J. HOWARD, *J. Chem. Phys.* **63,** 4212–4216 (1975).
6. S. SAITO, *J. Mol. Spectrosc.* **65,** 229–238 (1977).
7. C. E. BARNES, J. M. BROWN, A. CARRINGTON, J. PINKSTONE, AND T. J. SEARS, *J. Mol. Spectrosc.* **72,** 86–101 (1978).
8. H. PICKETT, private communication.
9. P. HELMINGER, F. C. DE LUCIA, AND W. GORDY, *Phys. Rev. Lett.* **25,** 1397–1399 (1970).
10. F. C. DE LUCIA, R. L. COOK, P. HELMINGER, AND W. GORDY, *J. Chem. Phys.* **55,** 5334–5339 (1971).
11. R. L. COOK, F. C. DE LUCIA, AND P. HELMINGER, *J. Mol. Spectrosc.* **41,** 123–136 (1972).
12. J. K. G. WATSON, *J. Mol. Spectrosc.* **65,** 123–133 (1977).
13. J. H. VAN VLECK, *Rev. Mod. Phys.* **23,** 213–227 (1951).
14. W. T. RAYNES, *J. Chem. Phys.* **41,** 3020–3032 (1964).
15. C. M. WOODMAN, *J. Mol. Spectrosc.* **33,** 311–344 (1970).
16. I. C. BOWATER, J. M. BROWN, AND A. CARRINGTON, *Proc. R. Soc. London A* **333,** 265–287 (1973).
17. J. M. BROWN AND T. J. SEARS, *J. Mol. Spectrosc.* **75,** 111–133 (1979).
18. W. C. BOWMAN AND F. C. DE LUCIA, submitted for publication.